Journal of Applied Research in Water and Wastewater
E-ISSN: 2476-6283
Journal homepage: https://arww.razi.ac.ir

Removal of lead and cadmium with an optimized composite of expanded graphite/g-C_3N_4/phenylenediamine

Mahboobeh Zarei[1], Majid Baghdadi [2,*], Fatemeh Yazdian[3], Naser Mehrdadi [2]

[1]Department of Environmental Engineering, Water and Wastewater, Kish International Campus, University of Tehran, Tehran, Iran.
[2]Department of Environmental Engineering, Graduate Faculty of Envirenment, University of Tehran, Tehran, Iran.
[3]Department of Life Science Engineering, Faculty of New Science and Technology, University of Tehran, Tehran, Iran.

GRAPHICAL ABSTRACT

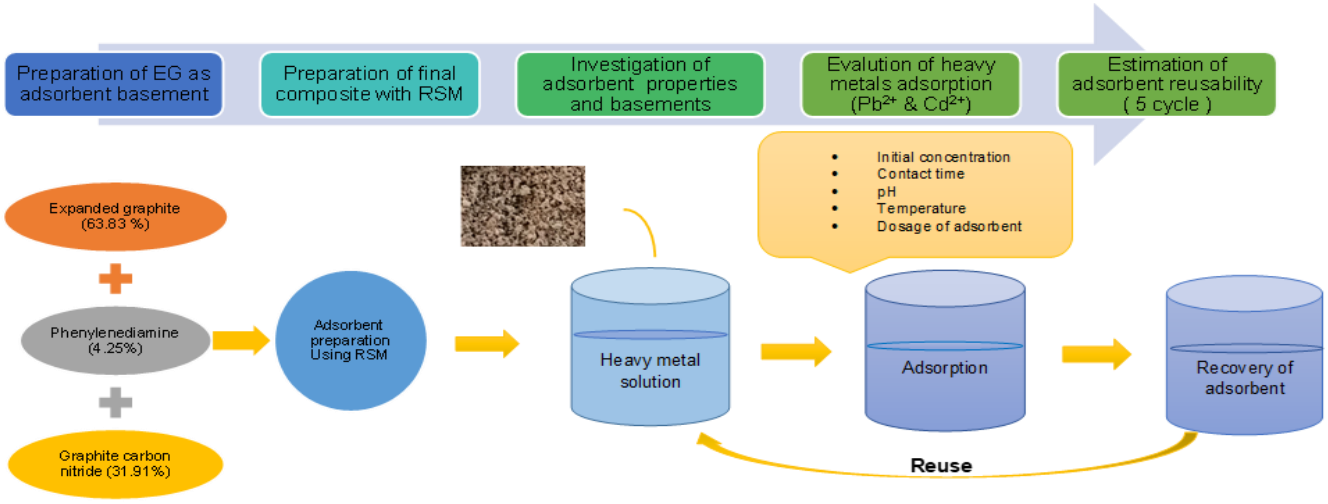

ARTICLE INFO

Article history:
Received 2 August 2022
Reviewed 1 October 2022
Received in revised form 4 November 2022
Accepted 5 December 2022
Available 7 December 2022

Keywords:
Response surface methodology
Expanded graphite
Adsorption
Cadmium
Lead

Article type: Research Article

ABSTRACT

In this study, an optimized composite of expanded graphite /g-C_3N_4 /phenylenediamine was synthesized and characterized by SEM, FESEM, EDS, XRD, and BET methods.The composite was prepared with an optimized combination using response surface methodology (RSM) as a proper adsorbent for eliminating heavy metals from water samples. The evaluation of the final adsorbent was accomplished by removing metal ions like Pb^{2+} and Cd^{2+}. Under the optimum adsorption conditions for Pb^{2+} and Cd^{2+} (pH:5, adsorbent dosage:2 g/L, and Time:60 min), elimination efficiencies were 78.4% for Cd^{2+} and 71.35% for Pb^{2+}. pH was the most important factor that influenced the adsorption rate. A short contact time for maximum removal efficiency was reported because of the porous structure of the constructed composite. As a result of the absorptive construction, the equilibrium showed a satisfactory agreement with the Freundlich model. The kinetic evaluations showed that the adsorption process of both heavy metals fitted the pseudo-second-order model. Furthermore, the results of thermodynamic studies indicated that the adsorption was an endothermic and spontaneous process. A series of regeneration experiments (5 cycles) was directed to evaluate the adsorbent reusability. The results presented that it was a suitable adsorbent for heavy metal uptake from aquatic solutions.

1. Introduction

The massive distribution of contaminants, such as heavy metals, in water sources has become a vital issue in the modern world. It is evident that industrial growth has caused countless environmental damages all over the planet, and the numerous solutions suggested by all experts are insufficient. Heavy metals have been considered highly harmful environmental impurities, poisonous to humans even at low concentrations, and possibly can cause enduring diseases (Duan et al. 2020). Development and extreme human activities have caused environmental pollution by harmful metals, even though these metals can naturally exist in the earth's crust (Tahoon et al. 2020). When heavy metal ions enter the water, they can be in different forms, such as cations, anions, and hydroxide complexes (Fergusson. 2015). Industrial toxins commonly include cadmium (Cd), nickel (Ni), lead (Pb), copper (Cu), chromium (Cr), and zinc (Zn) compared to other metals. Among

*Corresponding author Email: m.baghdadi@ut.ac.ir

How to cite: M. Zarei, M. Baghdadi, F. Yazdian, N. Mehrdadi. Removal of Lead and Cadmium with an optimized composite of expanded graphite/g-C_3N_4 /phenylenediamine using RSM , *Journal of Applied Research in Water and Wastewater* , 9 (2), 2022, 54-66.

these heavy metals, lead and cadmium have high adverse effects on humans in case of continuous exposure. These heavy metals can cause aquatic diseases, and the contaminated water can tremendously harm the ecosystem and humans. Therefore, it is essential to eliminate these contaminants from polluted water. World Health Organization (WHO) has the maximum contaminant level of 1.0 mg/L for lead and 0.1 mg/L for cadmium discharging into the surface water environment. Lead can adversely affect the hematopoietic, brain, gastrointestinal tract, and immune systems. In the case of cadmium, it is reported that it can cause Itai–Itai disease, kidney damage, renal disorder, and prostate or lung cancer (Chakraborty et al. 2020; Farimaniraad et al. 2021).

Up to now, many appropriate techniques have been applied to eliminate heavy metals from aquatic solutions. For instance, ion exchange, nanomembrane technology, and chemical precipitation are successful methods (Hadiani et al. 2018). Cations are replaced with metal ions in the wastewater during the ion exchange process. Different synthetic resins or natural zeolites are frequently used (Zhang et al. 2019). Some weaknesses of this method are the significant effect of the pH solution and its unavailability on a large scale (Chakraborty et al. 2020). In the membrane separation procedure, different membranes are used based on the pore size, but the process suffers from the drawback of high maintenance and operational cost. (Wadhawan et al. 2020). Chemical precipitation is another commonly used conventional process for removing various pollutants from contaminated water. There are also disadvantages when using this technique; for example, the requirement of an additional volume of chemical reagents for heavy metal removal, the production of a large quantity of sludge, and the high cost of sludge disposal (Argun et al. 2007). New materials applied in simple techniques like adsorption would be able to control pollution effectively (Negarestani et al. 2022). Adsorption has gained interest due to its low cost and environmental friendliness (Kheradmand et al. 2022).

New generations of adsorbents with higher efficiencies and low costs can be produced using nanotechnology. This development can lead to properly separating contaminants, including heavy metals (Chakraborty et al. 2020; Tahoon et al. 2020). A valuable element like carbon is widely used to create new adsorbents. The carbon derivatives' unique structure and constructional flexibilities are incredibly remarkable and make them a perfect resource for new composite materials (Taherian. 2019). Graphene oxides and expanded graphite are carbon-based adsorbents used for heavy metal removal. (Liao et al. 2017; Tahoon et al. 2020; Wadhawan et al. 2020).

Expanded graphite (EG) is a novel, efficient carbon material with a vast surface area, high mechanical power, and excellent electrical conductivity. Different procedures have been employed to produce EG, such as the quick heating of graphite to about 800°–1000°C, ultrasound irradiation, or microwave radiation (Hung et al. 2018). EG is mainly used in manufacturing gaskets, electrochemical processes, and thermal insulators. It is also identified as a perfect adsorbent material (Taherian. 2019). As many articles explain, expanded graphite composites (EG) are new carbon-based materials with significant potential usage in energy storage components, thermal insulators, fire-resistant composites, water treatment adsorbents, etc. (Liao et al. 2017). The electrical conductivity of EG was like graphite, but its expansion was more than 150 times (Liao et al. 2017). The proper incorporation of macromolecules in the interlayer space of expanded graphite can result in functionalized expanded nanocomposites, which can be efficient in heavy metal adsorption (Hung et al. 2018; Taherian. 2019). Graphite carbon nitride (g-C_3N_4) is an effective adsorbent with aromatic tri-s-triazine units that have been used to eliminate heavy metal and organic pollutants. Surface functionalization methods are available to expand the adsorption ability and reproducibility of the g-C_3N_4 (Sun et al., 2016). Melamine has been used as an excellent flame retardant because its structure has high nitrogen content. The application of this material in the development of different composites for g-C_3N_4 has been reported with perfect results. Polycondensation of melamine occurs at an increased temperature, forming a reactive resinous structure. This reaction results in the formation of a resin and then leads to its gelation (GŁOWACZ. 2013). Several researchers have tried to study coating materials on the surface, such as tin dioxide, conductive polymers, polyaniline, and phenylenediamine, to improve the eliminating properties (Taherian. 2019). Based on the new findings, different components can produce massive modified products. The surface functional groups attached to the carbon adsorbents were found to be responsible for the diversity in the physicochemical properties of these materials. Consequently, some studies focused on modifying and characterizing the surface functional groups of carbon composites to progress or extend their practical applications (Shen et al. 2008).

Phenylenediamine is an organic compound with the formulation of $(C_6H_5)_2NH$. It is a derivative of aniline, consisting of two amine groups bonded to a phenyl group. Due to its unique conjugated construction with amino groups, phenylenediamine can react with the oxygen-containing functional groups of the composite. It can accomplish functionalization and cross-linking reaction at the same time. Recently, the usage of this substantial element as a coating material has been developed for improving the adsorption capacity of new composite (Wadhawan et al. 2020).

In the present work, a new composite from two carbon sources was prepared to find optimal conditions for removing two heavy metals (Pb^{2+} and Cd^{2+}). The chemical structures of EG and g-C3N4 are highly different, which can improve the properties of the final adsorbent. Phenylenediamine was used as a coating material to enhance the adsorption capacity toward metal ions because this element affects the adsorption efficiency. The simple separation of the proposed adsorbent, a low production cast, and comparable uptake results will be advantages of prepared new composite.

2. Materials and methods

2.1. Materials

Graphite flask, sulfuric acid (98 % w/w), potassium permanganate ($KMnO_4$), and sodium hydroxide (H_2O_2 30% w) were obtained from Merck (Germany). The initial pH of the solution was adjusted by NaOH and HCl solutions (0.5 mole/L). The standard solutions of Cd(II) and Pb(II) with a concentration of 1000 mg/L were prepared by dissolving a certain amount of $Cd(NO_3)_2$ and $Pb(NO_3)_2$ in the deionized water. Deionized water (DI) was used for the entire experiment. The adsorption experiments in batch form were used to calculate the effects of adsorption parameters and optimal uptake of heavy metals. The common adsorbents applied for the deduction of heavy metals were in the form of powder. Therefore, their application was challenging, and the separation process from the solution in batch systems was satisfactory. A set of 100 mL of stoppered conical flasks containing 50 mL of solution and a definite amount of adsorbent was stirred at 150 rpm for a specific time until equilibrium occurred. Then, each tester was filtered individually over a 0.45 µm membrane to take out the adsorbent. The UV-vis spectrophotometer method analyzed the metal concentration evaluation before and after the process (Burakov et al. 2014). The experience was promoted with a fixed-speed stirring for almost 2 hours. The adsorbent mass used in each sample was 30 mg of composite for 0.05 L metal solution. After a specific time, a small selection (5 ml) of all flasks was filtered individually and diluted for spectrophotometer analysis (Burakov et al. 2014). In some tests, the number of samples for estimating the process behavior was additional (like the contact time section). Therefore, the experiment had a higher solution volume (200 mL), and the adsorbent weightiness was also upper (0.12 g).

2.2. preparation of expanded graphite

One-step rapid preparation of EG can provide an enormous amount of adsorbent at room temperature. The mixture of natural graphite with nitric acid and sulfuric acid generally produces expandable graphite. The present work used a combination of H_2SO_4 (77.5%) and $KMnO_4$. 20 mL of the concentrated sulfuric acid, which acted as the intercalant, and 1.5 g of $KMnO_4$ was stirred at ambient temperature for 10 minutes. Then, a certain amount of flake graphite (1 g) was gradually mixed with the prepared solution. After a specific time (almost 120 minutes), the intercalation process was completed. Then, 10 mL of H_2O_2 was added slowly. After 24 hours, the obtained EG was washed with deionized water, filtrated, and dried in an oven at 60°C for 1 hour (Hou et al. 2020). Adding H_2O_2 caused a significant modification in the composite structure (THUONG et al. 2019). Then, the mixture was washed with deionized water, filtered, and dried in the oven at low temperatures (Liu et al. 2017).

2.3. Preparation of the composite

At first, the adsorbent synthesis procedure was optimized by using a design expert. Subsequently, lower material consumption and fewer tests are required. In the present work, RSM based on the Box-Behnken method (BBD) using design expert software (Version 11.1.0.1) was needed to adjust the weight of different components in the final product. Response surface methodology (RSM) is a beneficial tool in investigating the interactions between the variables in a system and calculating the optimal situations. This program contains

experimental methods to estimate the connection between several variables and responses (Yuan et al. 2019).

One of the RSM subgroups is the Box-Behnken design (BBD), similarly identified as the three k-p design, which includes 3-level factors and interaction terms (Parmar et al. 2020). It can provide a significant analysis performance to detect the consequence of independent variables on the removal efficiency of the metal ions with a smaller number of trial runs equally compared to CCD, which is frequently chosen for optimizing variables. The fewer experiments in BBD make this model a reasonable alternative to CCD (Yuan et al. 2019). According to various articles, selecting a suitable ratio of components is hugely vital, considering their role in the final product structure and properties. It is possible that the modification ultimately caused the reduction of specific surface area. The total number of surface functional groups improved the adsorption of impurities (Shen et al. 2008). The main components of the composite were Expanded Graphite (EG), Graphite Carbon Nitride (g-C_3N_4), and diphenylamine (Meibodi and Soori. 2022). To predict the optimized conditions correctly and diminish the tests, the Box-Behnken design (BBD) was beneficial. The selected substructure components' mass is a critical factor that influences the properties of the adsorbent, such as adsorption capacity. The range of each material is shown below:

I. (Weight of Expanded Graphite as a basement): 0 – 30 g
II. (Weight of Melamine for preparing g-C_3N_4): 0 – 15 g
III. (Weight of phenylenediamine as a coating material): 0 – 2 g

The different dosages of the elements are presented in Table 1.

Table 1. RSM design values for optimization of the composite.

Run	Variables			Response 1 Heavy metal (Nickle) uptake
	A: Expanded graphite	B: Melamine	C: Phenylenediamine	
	g	**g**	**g**	**%**
1	15	0	2	65.58
2	30	0	1	67.19
3	15	7.5	1	70.1
4	30	7.5	2	66.17
5	15	7.5	1	75.05
6	15	15	2	68.15
7	0	7.5	0	54.12
8	30	15	1	62.45
9	0	7.5	2	45.13
10	30	7.5	0	60.45
11	15	7.5	1	74.96
12	15	7.5	1	73.22
13	15	15	0	63.33
14	15	0	0	60.55
15	0	15	1	53.2
16	0	0	1	50
17	15	7.5	1	65.6

The experimental data showed that the increase in the mass of expanded graphite in the composite could cause a greater uptake rate. Therefore, a reliable ratio of elements was selected, and a specific range for three parameters was employed. The chosen model must have an insignificant lack of fit. The ANOVA section determined the influencing factors for the model suitability. The descriptive statistics and statistical tests are also presented in the ANOVA table (Table S1).

Generally, p-values are investigated to find the significant model terms. Analysis of Variance is based on the p-values to control if the model is a considerable portion of the variance. With some extra runs and replicates, a lack-of-fit test will be delivered. Summary Statistics show the expressive statistics used as a secondary pattern for the model utility. The Predicted R-Squared and Adjusted R-squared are vital parameters. The model fits the data if the difference is fewer than 0.2. Adequate Precision is also a critical parameter. If it is larger than four, the model has enough signal for optimization. The F-value was 9.31, which reveals the significance of the model. It was only a 0.38% coincidence that such an F-value could happen due to the noise. P-values fewer than 0.0500 showed the essential parts of the model. In this example, A, A^2, and C^2 are significant. Values larger than 0.1000 showed that the model terms were not practical. The Lack of Fit of 0.58 indicated that F-value was insignificant compared to the pure error. There was a 66.12% chance that a Lack of Fit for this large F-value could occur due to the noise. Pay attention that a non-significant lack of fit is good. Adequate Precision measures the signal-to-noise ratio. A ratio of more than 4 was necessary. So, the amount of 8.982 showed a suitable signal. This model can be applied to direct the design space. CV% was used in some activities to criticize the ability of the process, and a minor quantity was more valuable. Comparison of the standard deviation was also essential to evaluate a model's efficiency.

According to the results, the highest efficiency was achieved by the specific proportion of constituent materials.

R^2 = 0.9229
Adjusted R^2 = 0.8237
Predicted R^2 = 0.5439

2.4. Analysis of residual graphs

The analysis of residuals provides a more sophisticated method for determining a good fit of a regression model. It is valuable for several regressions where a Scatter Plot is unavailable for visual assessment. The study of normality was essential, and the plot of normal residuals displayed the accurate probability of the collected data. Based on the plot, a straight line could be a sign of normal distribution that is highly acceptable (Parmar et al. 2020). In the plot of predicted versus actual, the absolute standards were demonstrated by square marks. The predicted evaluations were in the form of a straight line, and additional accordance between these groups was highly satisfactory (Fig. 2).

The predicted versus actual removal percentage chart is also shown in Fig. 2. As mentioned previously, in this plot, the square marks are symbols of the actual values and are predicted as a straight line demonstrating quantities. An appropriate overlap between the predicted and actual amounts for replies is observed. The residual test (t-test) found outliers by assigning a t-value. An outlier must be a sign of a higher t-value.

Analysis of 3D response surface plot

In this section, the evaluation of the contour plot was critical. According to the plots, the highest adsorption efficiency occurred in a particular ratio of elements. The 3D surface charts were graphs of regression equations showing two foundations, whereas other elements conserved were fixed (Yuan et al. 2019). The proper ratio of the different components was close to the final results obtained from the experimental study (Figs. 1 and 3).

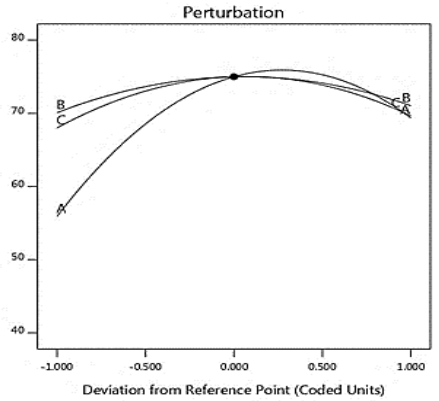

Expanded Graphite (Wet form): 15 g (63.83%)
g-C_3N_4 (Formed from melamine): 7.5 g (31.91%)
Phenylenediamine: 1g (4.25%)

Fig. 1. Substantial composite materials with a definite weight in the final adsorbent structure.

The optimal weight rate are presented in Fig.1. According to Table1, the extreme metal removal efficiency of 75.05 % is gained by using this weight rate in the composite preparation process.

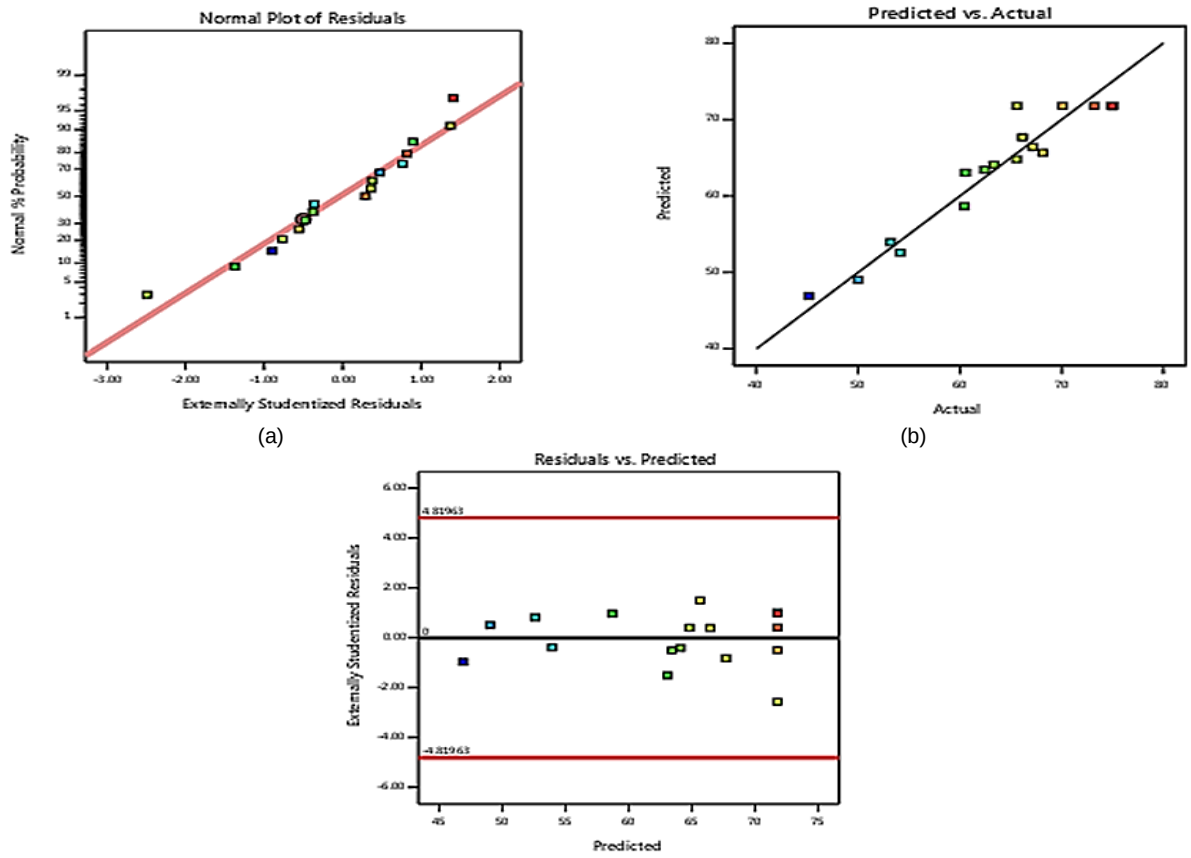

Fig. 2. Different residual graphs: normal plot of residuals (a) predicted vs. actual plot (b) and residual vs. predicted plot (c).

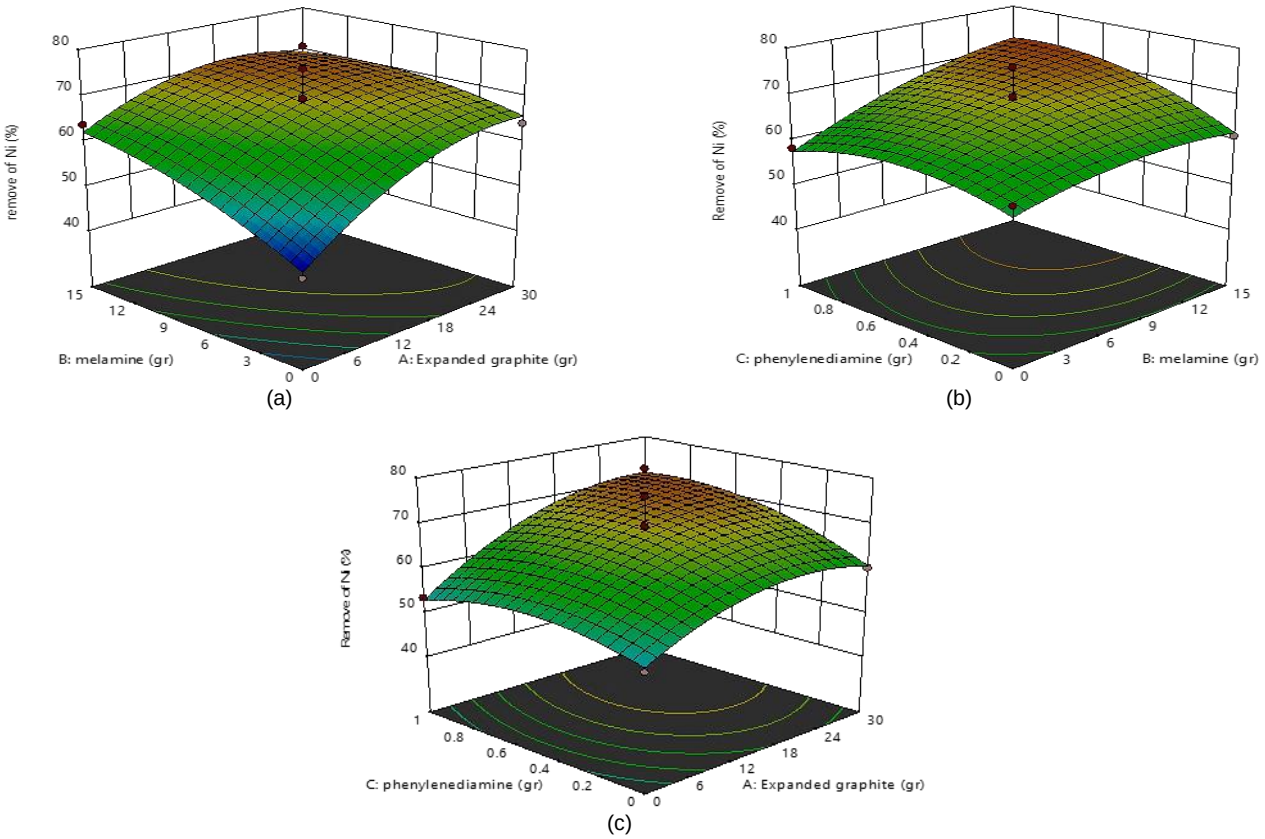

Fig. 3. Analysis of 3D responses about interaction of the composite components obtained by 3D plotting: (a) Expanded graphite vs. melamine, (b) melamine vs. phenylenediamine , (c) Expanded graphite vs. phenylenediamine.

2.5. Final equation in terms of coded factors and actual factors

Based on the design expert application, two variations were eventually estimated. One variation was related to the model, and the other was associated with the experimental errors. In that case, it is possible to control whether the variant from the model is significant or not. The last model was designed by estimating the F-value stated as the square-to-residual error fraction of the mean model. If the intended F-value was more than the tabulated one, then the model is a substantial trial data predictor (Bayuo et al. 2020). In the present study, the F-value was 9.31. (The final equation is presented in Table S2 with the model expressions.) The coded equation can be used separately to predict the response for a particular level. By default, the factors at high and low levels are coded as +1 and -1, respectively. The coded equation is valuable in finding the virtual effect of the elements by comparing the factor coefficients. The actual equation can be applied to evaluate the reaction for definite stages of each feature. The phases should be identified in the substantial components for elements individually, which are presented in Table S3. The primary role of EG in adsorbent properties is undeniable, and adding phenylenediamine was profitable for improving removal efficiency.

3. Characterization of adsorbent

3.1. Evaluation of scanning electron microscopy (SEM), field emission scanning (FESEM), and Energy Dispersive X-ray spectroscopy (EDS)

SEM analysis is a convenient evaluation instrument that uses a focused beam of electrons to produce functional, complex images of the sample surface. SEM analysis can reveal valuable information about the outer surface of composite structures, which might be approval of the metal ions adsorption (Shafiq et al., 2021). FESEM is also a tool that provides lots of information from the outside structure, but the resolution is higher, and a superior energy range is evaluated eventually (Abbas et al. 2017). FESEM scanned the out layer of material with an electron beam and monitored the data in the same way as SEM. The difference between SEM and FESEM analysis lies in the electron generation system. So, in the FESEM system, the spatial resolution enormously improves, and the charging effects are minimized evidently (Savaloni and Savari. 2018).

Generally, expanded graphite is a graphite basement construction that has a layered structure with interlayer spaces. The prepared sample showed an expanse structure that verified the composite foundation (Figs.5(c) and 5(d)). Forming a porous foundation was extremely valuable, as the number of active sites would ultimately rise. EDS or EDAX provides a different understanding of the composite surface during the SEM or FESEM process. EDS evaluation was used to acquire the elemental components of the material and provide more quantitative results (Mohanraj et al. 2019). The method of evaluating samples also took place in two groups: prepared expanded graphite (Composite foundation) and the final product. The ultimate composite combined expanded graphite and graphite carbon nitride with a coating layer of phenylenediamine for adsorption improvement. Fig. 4 confirms the estimation of EDS parameters for the prepared EG.

A) Prepared expanded graphite (composite basis)

According to the results in Fig. 4, the EDS examination presented that the external layer was typically composed of carbon and oxygen elements. Moreover, a small amount of nitrogen is also identified. The highest element weight rate belongs to carbon as a significant basement material (Fig. 4a), and the amount of oxygen is less than carbon. The minimal weight of nitrogen is also found.

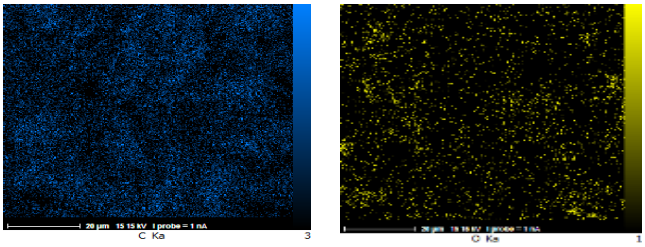

(a) (b)

Fig. 4. EDS spectrum pattern of the expanded graphite as the basement of adsorbent: (a) Carbon distribution - (b) Oxygen distribution.

Along with Fig. 5, the graphite structure changed from a scale to a worm-shaped format (Figs. 5a and b), and the morphology of the prepared EG surface displays a fine exfoliated formation that demonstrated steady extension. The moisture content of each sample is about 2% of the combined weight.

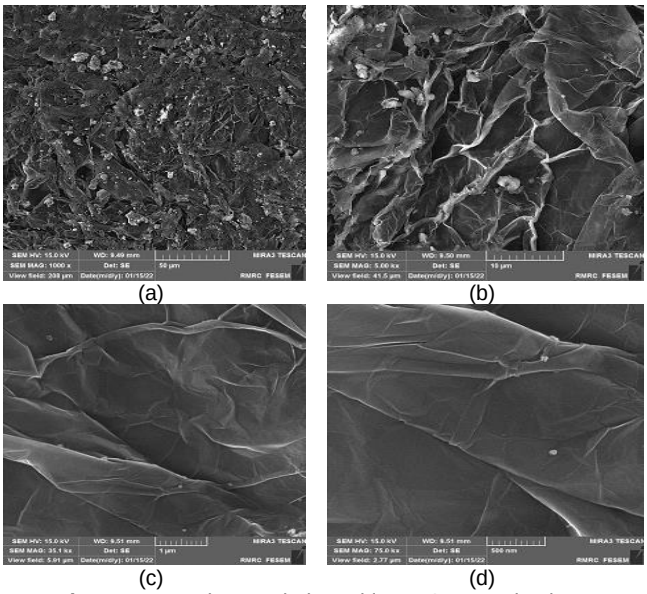

(a) (b)

(c) (d)

Fig. 5. Prepared expanded graphite FESEM evaluation.

B) The final composite

After mixing all substantial elements with specific mass weight**,** the final phase was performed using a programmable furnace at a particular heat (500°-550° C) for a definite time (180-300 min) without oxidation (Taherian. 2019). The SEM photos in Fig.6(b) demonstrate that additional elements are dispersed unequally among the sheets and on the external layer of the expanded graphite. The basic structure has changed to a wormed-like lumpy shape, but the cylindrical formation has remained consistent.

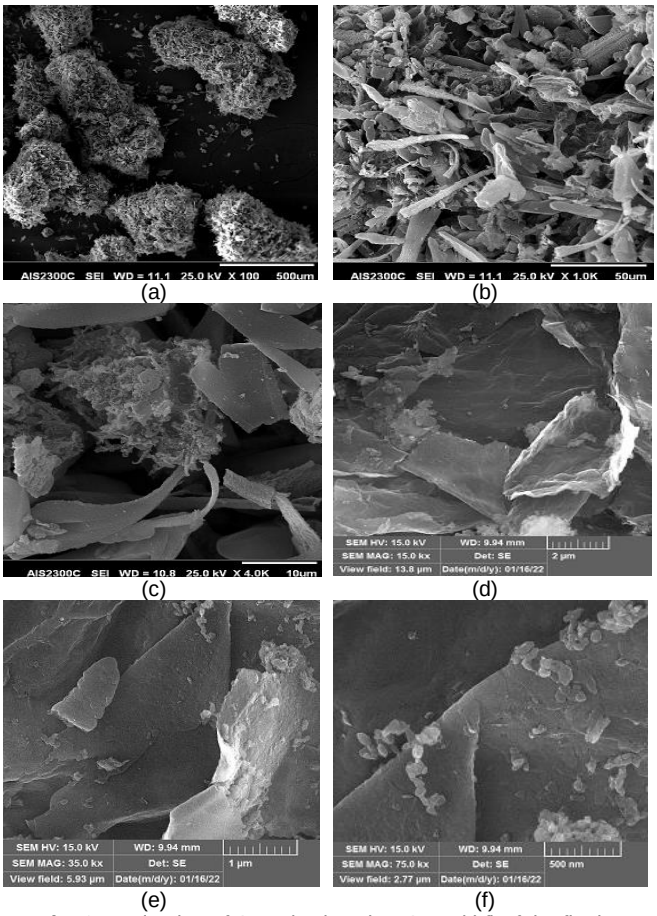

(a) (b)

(c) (d)

(e) (f)

Fig. 6. Evaluation of SEM (a-c) and FESEM (d-f) of the final composite.

Furthermore, it is evident that the space between layers is inflated, and the exfoliated area has a multi-sheet body with several spherical-shaped holes(Figs. 6(c) and 6(d)). The decomposition of g-C_3N_4 from melamine or phenylenediamine has released a white cover on graphite layers (Figs. 6(a) and 6(b)), but the worm shape of EG is noticeable. The existence of coating materials can enormously improve the uptake properties of the final composite as the new formations occur in porous parts (Figs. 6e and f). Based on the EDS spectrum in Fig. 7 (Table 2), the elemental composition confirmed the presence of other elements. The higher weight rates are ideally related to carbon and nitrogen (Fig. 8). The coating materials can undoubtedly improve the existence of nitrogen in the composite (Meibodi and Soori. 2022).

3.2. X-ray powder diffraction (XRD) and The Bruner–Emmett–Teller (BET) analysis

The diffraction of X-ray powder is a rapid analytical system that is used for segment identification of composite. It can provide valuable information on unit cell dimensions (Fig. 9). This method is robust and rapid (less than 20 minutes) for detecting unknown materials. The computerized XRD instrument includes a monochromatic energy foundation and stepping engine (Gupta et al. 2022). The articles predicted the possibility of two vast peaks at 21.8° and 43.7° for graphite (Mohanraj et al. 2019).

Table 2. Table of the final composite element content.

Elt	W%	A%
C	45.19	49.53
N	51.68	48.58
O	1.58	1.30
S	1	0.41

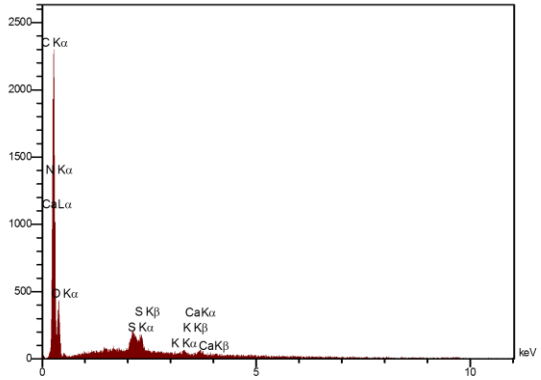

Fig. 7. EDS spectrum patterns of the final composite.

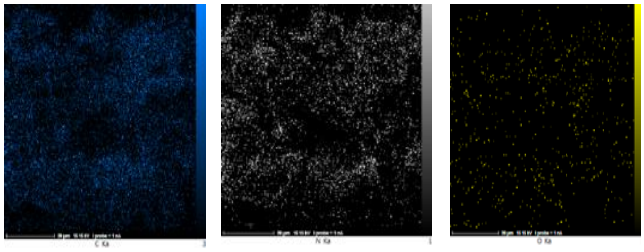

(a) (b) (c)

Fig . 8. The element content of the composite, (a) Carbon distribution, (b) Nitrogen distribution, (c) Oxygen distribution.

According to the XRD analysis in Fig. 9, the sharp and intensive diffraction peak of the final product at 27.8° corresponds to EG for the basement elements composite. A small diffraction peak of the composite at 13.08° has appeared, mainly because of the g-C_3N_4 formation on the expanded graphite structure. It indicates that the basement contracture and final composite consist of microcrystalline graphite with a layering structure, and the orientation of the graphite sheets did not change much (Celzard et al. 2005).

The diffraction peak width is a significant factor in XRD analysis that might demonstrate microstructural information. The peak growth is not quantified when the crystallization size is larger than the extreme limit. The structure of g-C_3N_4 inside the composite was considerable.

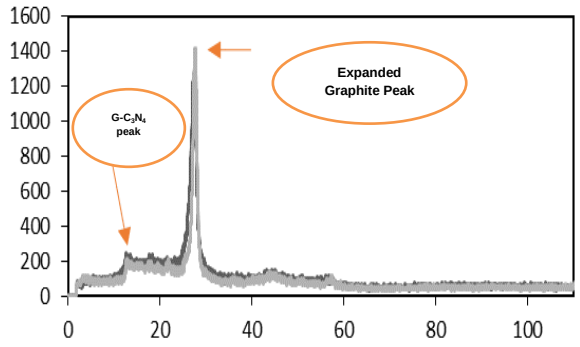

Fig. 9. XRD analysis of the main elements of the composite and the final adsorbent.

BET analysis has esteemed the sample-specific surface area (Falsafi et al. 2020). The nitrogen adsorption data (N2 adsorption-desorption apparatus) was used to define the BET surface area (SBET), the total pore volume (Vtot), and the microspore volume (Vmic) of the composite (Jiao et al. 2017). The BET surface was established by using the BET equation to the adsorption data obtained over the P /P_0 ambit 0.10–0.1, V_{tot} gained from the total adsorption was measured at P/ P_0 = 0.99. At the same time, the microspore volume, V_{mic}, was achieved using the t-plot scheme (Table 3) (Nouri. 2003).

Table 3. BET Analysis of the final composite.

Spesific surface area	Total pore volume	Mean pore diameter
23.791 m^2/g	0.1488 cm^3/g	25.019 nm

The results showed that the specific surface area is close to other outcomes (22.4 m^2/g), and the determined pore volume was less than graphite values. This might be due to the comparative mass of the nitrogen molecules inside the composite structure (because of adding melamine). It was suggested that the smaller N_2 molecules could search microspores inaccessible for the phenylenediamine. The reduction in porosity causes the decrease of specific surface area, as evidenced by BET analysis (Bannov et al. 2021; Falsafi et al. 2020).

3.3. Adsorption experiments

The result evaluation was performed by the removal percentage, which showed the volume of adsorbed metal ions after a particular time. The removal efficiency fraction was calculated using Eq. 1: (Tang et al. 2017).

$$R = \frac{(Co-Ce)}{Co} \times 100 \quad (1)$$

where, C_o(mg/L) is the concentration at the beginning of the experiment and C_e(mg/L) shows the equilibrium concentration of the solution (Liao et al. 2017). The volume of heavy metal adsorbed at equilibrium (q_e) was calculated by Eq. 2 (Chen. 2015).

$$q_e = \frac{(C_o - C_e)\times V}{m} \quad (2)$$

where, C_o and C_e (mg /L) are the initial and equilibrium concentrations of the solution, V (L) is the volume, and m (g) is the adsorbent mass used for each sample (Tang et al. 2017).

The optimal condition was investigated by studying the effect of pH, contact time, initial concentration of metal ions, and adsorbent mass on the removal efficiency to reach the optimal removal rate and adsorption capacity. The metal ion's elimination examined different adsorption isotherms in the optimal condition.

3.3.1. The effect of pH

In general, adsorption is a physical-chemical procedure that involves several restrictions. Each of these parameters, such as pH, can cause unlimited changes. According to various studies, pH is the most critical parameter that can change the amount of heavy metal ions uptake from aqueous solutions (Nouri. 2003). pH not only affects the efficiency of the process but also can influence the surface chemistry of sorbent and modifies the metal ion specifications. It is reported that not all metal ions behave similarly at the same pH. Therefore, finding an optimum value for pH can promote maximum removal efficiency, ultimately reducing operational costs. (Cruz-Lopes et al. 2021). In solutions with low pH values, due to the electrostatic interactions between practical protonic sections on the surface and metal ions, the

chemical balance of the reagents changes eventually. It can also cause a slowdown of separation.

On the other hand, the large amount of H^+ and H_3O^- ions in water prevents the adsorption of other ions and reduces the retention rate. On the contrary, in solutions with high pH values, the electrostatic forces are vastly reduced, which causes the activation of protonation sites and increases the adsorption rate (Wadhawan et al. 2020).

According to many studies about lead uptake, the possibility of sediment was high in pH values higher than 5.0. Thus, the ideal pH for removing Pb^{2+} from water should be less. Some solutions in the range of 2.0 to 5.0 are required for evaluating a suitable pH value. The adjustment of the exact pH value was promoted by the hydrochloric acid (0.1 M) and sodium hydroxide (0.1 M). Besides, other factors such as temperature, were kept constant to avoid interference. (Liu et al. 2013). The experiments with various pH values were conducted to determine the optimum pH value, and its effect on removal efficiency and adsorption capacity was investigated. During the experiments, other parameters were kept fixed.

Based on the results of the contaminant uptake shown in Fig. 10, the solution pH is a very imperative factor in the vibes of the metal ions, their struggle for the binding sites, and the functional groups' movement on the adsorbent surface (Liu et al., 2017). The results show different percentages of Pb^{2+} and Cd^{2+} removal from the solution. Based on the experiment results, the highest uptake occurs at pH=5. Obviously, the initial phase of elimination in every sample sharply increases with the higher sum of active sites. Then, the speed of the process turns slow. The quantity of separated ions becomes stable, which is a clear sign of equilibrium.

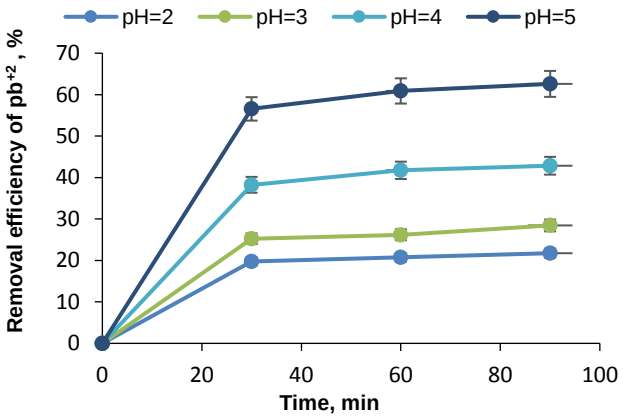

Fig. 10. The values of removal efficiency in different pH values for adsorption of Pb^{2+}(a) – Cd^{2+}(b) with initial concentration of 30 ppm, contact time of 0 to 90 min, under the ambient temperature.

As shown in Fig. 10, the optimal pH value plays a vital role in achieving higher metal ion removal efficiency. The growth of qe in higher pH values is significant as the concentration of all samples was identical, and the adsorption rate of two contaminants increased (Fig.11). The evaluation of the final pH indicated that altered pH values of each sample caused a slight alteration in the adsorption process that could be due to the cation exchange mechanism (Darweesh et al. 2022). It is suggested that the uptake rate remains constant afterward, indicating that Cd^{2+} or Pb^{2+} removal is favored at moderate values because of functional group deprotonation that reduces repulsion powers. Hence, the composite adsorption capability is inside the molecular construction and depends on the solutions' electron density (Tahoon et al. 2020; Wadhawan et al. 2020). The minor deduction of metals in the acidic solution results from the competition between H^+ and repulsive forces of the surface with cationic metal ions. Therefore, a lower electrostatic repulsion with diminished adsorbent capacity happens at low pH (Cruz-Lopes et al. 2021).

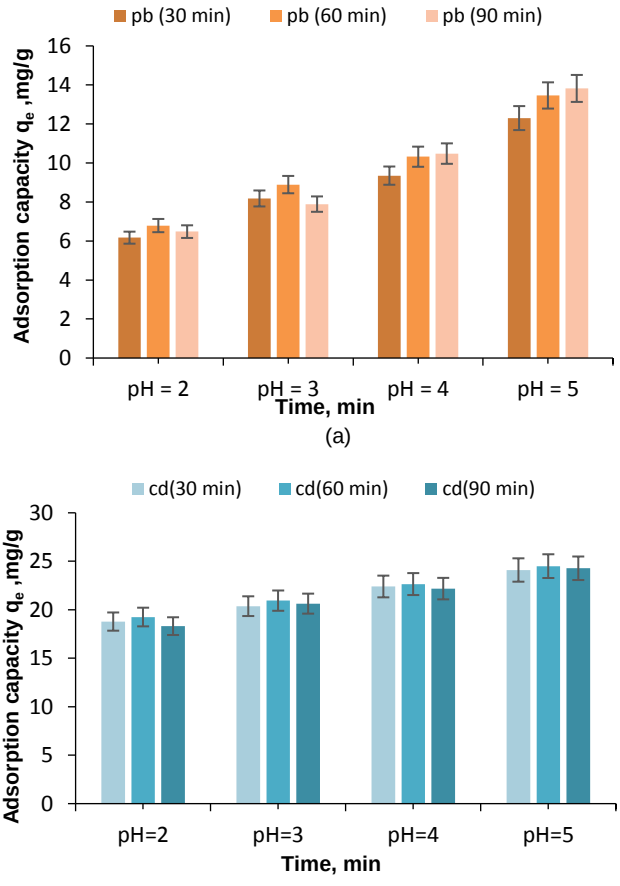

Fig. 11. Evaluation of qe in different pH for Pb^{2+} (a) – Cd^{2+} (b) metal ion uptakes with initial concentration sample of 30 mg/L, contact time of 0 -60- 90 min, under the ambient temperature.

The results showed that the adsorption capacity of Cd was better than Pb, especially when the initial solution pH was higher (Fig.11). The results were similar to other articles, and the solution's initial pH in the remaining experiments was chosen as 5 (Hadiani et al. 2018; Tang et al. 2017).

3.3.2. The effect of initial concentration of heavy metal solutions

Generally, any contaminant's high concentration could result in a positive movement force for removing pollutants in the adsorption method. So, higher initial concentrations of heavy metal ions can improve the adsorption uptake (Jiao et al. 2017). The optimization of initial concentration provoked a perfect situation for further elimination of metal ions and reduction of additional operation charges. So, the evaluation of initial concentration is essential. For this purpose, the effect of concentration was examined in different samples with diverse substances of Pb^{2+} and Cd^{2+}. According to Fig.12, the removal efficiency increased in higher concentrations, and the equilibrium phase occurred ultimately. At the beginning of the adsorption process, the uptake rate increased sharply, corresponding to numerous blank active sites on the composite surface. However, an additional rise showed negative consequences owing to the limited number of offered adsorbent sites. The amount of removal efficiency for higher concentrations was close. This behavior might be due to the adsorbent's limited ability or accomplishment of all active sites. It is a fact that the number of metal ions in low concentrations was fewer than in active positions on the external layer, which conducted the lower adsorption rate (Shafiq et al. 2021). Similar results were reported for carbonyl composite by different investigators (Hadiani et al. 2018; Imran Ali et al. 2018). The grades confirmed that this composite could

remove low concentrations of lead and cadmium, which is valuable for reducing drinking water or industrial wastewater pollution. The initial concentration of other sections was selected as 30 mg/l to achieve more significant uptake results (Abdulkarim and Al-Rub. 2003).

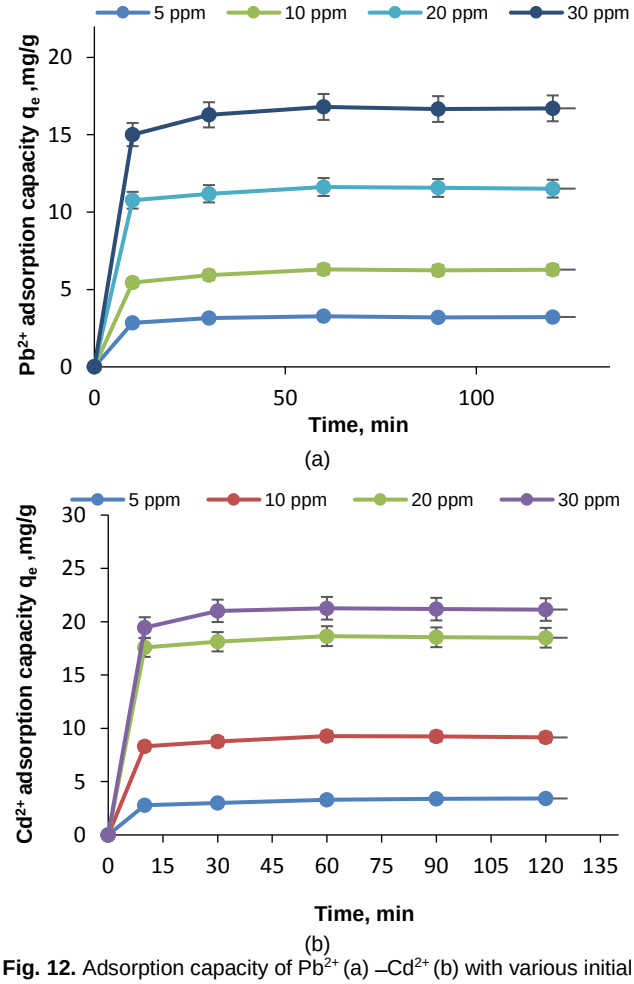

Fig. 12. Adsorption capacity of Pb^{2+} (a) –Cd^{2+} (b) with various initial concentration samples of 5-30 (ppm), pH=5, contact time of 0 to 120 min, under the ambient temperature.

3.3.3. The effect of contact time

The contact time between metal ions in the solution and the surface of the adsorbent is a significant element in the process optimization. Numerous studies have attempted to explain the connection between time and removal efficiency, showing that the separation rate augments with time passing (Abdulkarim and Al-Rub. 2003; Jiao et al. 2017). It is a fact that during the initial section of the process, a remarkable increase occurred in removal efficiency. Consequently, the procedure becomes slower (Jin et al. 2015). Logically, the speed of removing the particles should be high in the beginning, considering many spare surface-active sites. Because of the equilibrium, there would be a balance inside different parts, and the operation will become time-independent. It means that the adsorption and desorption speeds become even.

Subsequently, the study of contact time was a way of finding the optimum condition for the adsorption process. Many elements, such as the property of adsorbent and metal ions, adsorbent dosage, etc., influence equilibrium (Rao et al. 2003). Furthermore, the impression of this factor on the kinetic model was indisputable. In this part, the effect of contact time on the adsorption process was estimated by the upper volume of solution (200 mL) as the number of required samples was more than in the previous sections.

According to Fig.13, the equilibrium happened shortly after the beginning of the experiment, but the amount of q_e became constant after 60 mins. So, 60 min was selected as a suitable contact time for eliminating both contaminants. The result also revealed that the removal efficiency of both pollutants was almost identical. However, the q_e values were notably different at the beginning of the process. It was clear that the removal development was speedy. In addition, the equilibrium occurred before 60 mins. As mentioned in several articles, the initial removal efficiency of metal ions was rapidly increased in the time range of 0-90 min and then approached equilibrium (Imran Ali et al 2018 - Ocreto et al. 2019). Fig.13 showed similar consequences of the contact time of 60 min. So, 60 min was selected as the optimum equilibrium time for the other sections.

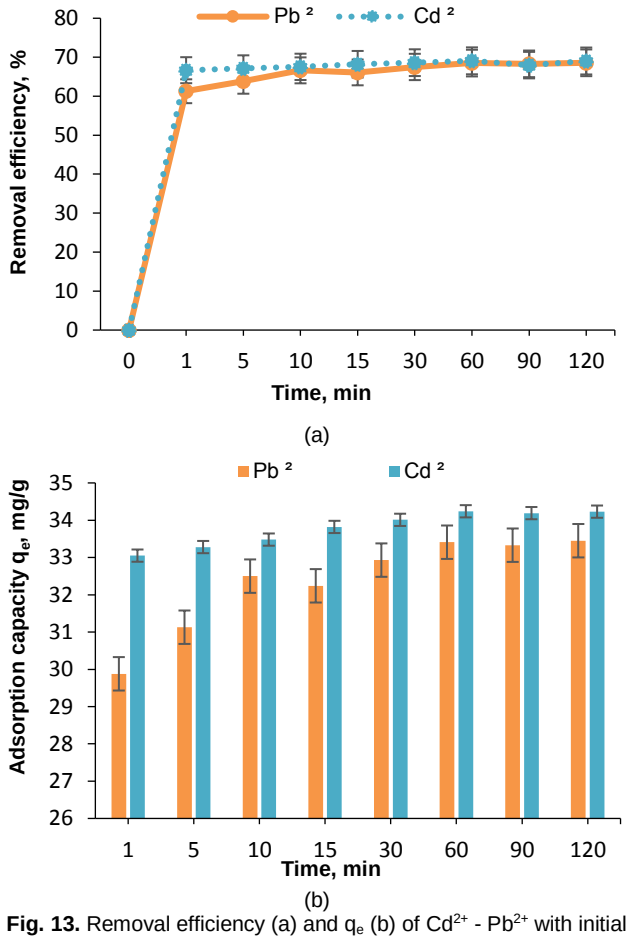

Fig. 13. Removal efficiency (a) and q_e (b) of Cd^{2+} - Pb^{2+} with initial concentration of 30 ppm, pH=5, contact time of 0 to 120 min, under the ambient temperature.

3.3.4. The effect of temperature

Several studies illustrated that temperature is one of the principal factors in different interactions, as the alteration of energy can significantly impact the speed and products. It is a fact that changing temperature is a way of developing the quantity, movement, and dispersion rate of ions. Therefore, at a higher temperature, the adsorption efficiency possibly rises (AbdulKarim and Al-Rub. 2003). Beforehand, any temperature changes could affect the procedure in two forms that depend on the nature of interaction and the estimation of the heat evaluation. So, the initial temperature rise diminished the solution viscosity. Then, this led to the development of the dispersion rate of the contaminant molecules through the out layer and ended in higher adsorption effectiveness.

The temperature variation can disturb the adsorption procedure in two different behaviors, depending on the process nature, whether it includes absorption or desorption of heat. The two models of chemical operations are known as exothermic and endothermic mechanisms. The rate of adsorption in exothermic procedures increases notably with the diminishment of temperature. In contrast, the endothermic processes demonstrate a higher removal rate for temperature enhancement, which results from viscosity drop (Zhang et al. 2019). Furthermore, the grade of randomness at the solid-liquid interface improves in an aqueous solution (Imran Ali et al. 2018). The experiment occurs in different samples with a constant concentration of heavy metal solutions and distinct weights of adsorbent for an hour.

The adjustment of temperature completes with the heater before adding the adsorbent. The solution temperature in all samples was constant for the test duration. Based on Fig.14, The maximum uptake of both contaminants is evaluated in ambiance temperature. The increase in temperature reduced the removal efficiency. The

calculation of q_e similarly shows a decrease for both pollutants, and the highest removal rate also happened at ambient temperature.

According to the results, the adsorptive capacity was practically constant for removing the metal ions. The results showed that the removal of both metals was spontaneous and endothermic, and the environmental temperature was appropriate for the process (Imran Ali et al. 2018; Tang et al. 2017).

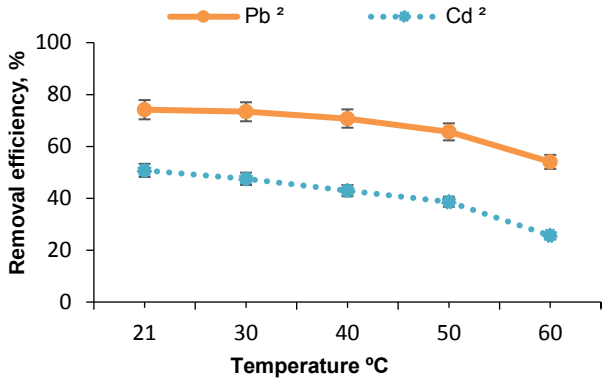

(a)

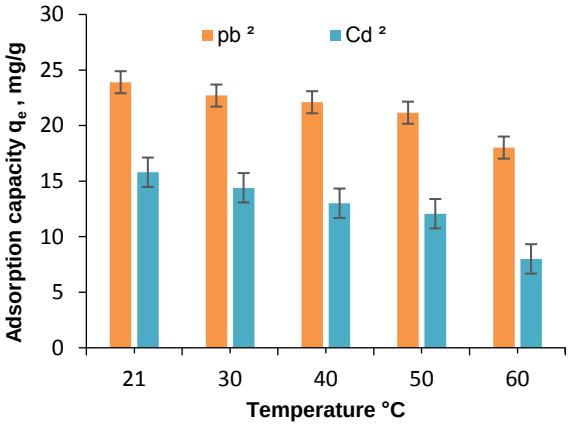

(b)

Fig.14. The effect of different temperatures on the removal efficiency (a) - q_e (b) of Cd^{2+} - Pb^{2+} with initial concentration of 30 ppm, pH=5, contact time of 60 min.

3.3.5. The effect of different dosages of adsorbent

The rise of adsorbent dosage in the process seems to lead to a better removal percentage since the more available surface area with additional active sites exists. On the other hand, it is evident that after reaching the equilibrium, more volume of adsorbent turned useless, and the rate of removal process remained constant. It is vital to choose a perfect dosage for reducing waste and achieving the highest removal efficiency (Liu et al. 2013).

It is also confirmed that the increment of adsorbent might cause particle accumulation, which induces the reduction of total surface area and raises the diffusion path length of heavy metals (Zhang et al. 2019). Besides, it is established that the removal rate never becomes 100% for any reaction due to metal ions' desorption in the solution or lower q_e value (Jin et al. 2015). In this part, the removal rate of metal ions is evaluated by different amounts of adsorbent dosage, and other parameters were all constant.

Logically, a higher dosage of adsorbent would provide more opportunity for the metal ions to be caught by the active sites on the adsorbents. However, the lower adsorbent dosage can lead to a higher adsorption capacity. This effect was based on the solute distribution between the adsorbent and bulk adsorbate solution. According to Fig.15, the impact of adsorbent dosage on the adsorption capacity is represented. The adsorption capacity has decreased by increasing the adsorbent dosage. However, the removal efficiency does not reach 100%, indicating that the participated adsorption of Cd^{2+} and Pb^{2+} between composite and solution has occurred. Therefore, adsorption and desorption exist in the system (Tang et al. 2017).

The results displayed that the removal efficiency of Cd^{2+} was increased from 42.45 % to 78.4 %, and the rise of Pb^{2+} removal was more than 17% with an adsorbent dosage rise from 0.01 to 0.1 g. Compared to other articles, similar results occurred, and the optimal adsorbent dosage was set to 2 g/L for removing Pb^{2+} and Cd^{2+} (Imran Ali et al. 2018; Parmar et al. 2020).

3.4. Adsorption isotherm

As identified by many researchers, the study of isotherms provides precious evidence about adsorbent capacity, adsorption mechanism, and also estimation of process achievement (Ocreto et al. 2019).

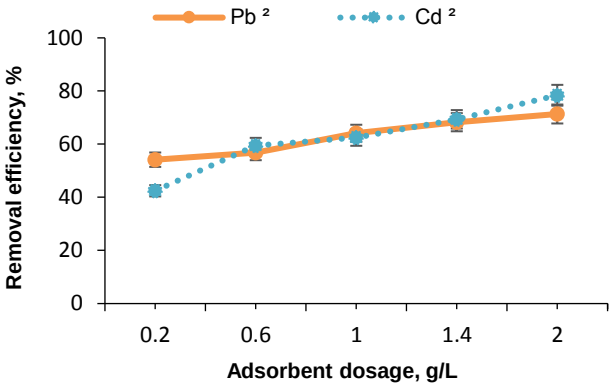

(a)

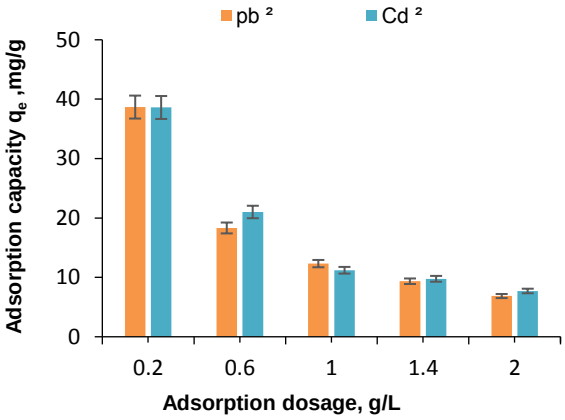

(b)

Fig.15. Effect of different dosages on removal efficiency (a) – q_e (b) with initial concentration=30 ppm, pH=5, contact time of 60 min, under the ambient temperature.

The adsorbent performance is evaluated by adsorption isotherm data, which can be attained by some experimental tests. Modeling the adsorption isotherm data is a necessary technique for calculating and comparing the adsorption parameters, which is essential for the adsorption mechani5sm path optimization, expression of the adsorption capacities, and functional design of the adsorption structures (Chen. 2015). Isotherm models like the Langmuir and Freundlich equations are frequently used to describe the adsorption data (Burakov et al. 2014). Langmuir model describes the monolayer ions adsorption on the adsorbent surface with a constant number of active sites related to component molecules (Dowlatshahi et al. 2014).

According to the models, the regression parameters and correlation coefficients (R^2) indicate that the adsorption data best fitted to which isotherm. The evaluation of different factors of two isotherms is presented in Table 4 (Figs. S1 and S2). The linear form of this model is presented in Eq. 3.

$$\frac{C_e}{q_e} = \frac{1}{q_{max} \times k_l} + \frac{C_e}{q_{max}} \quad (3)$$

The characteristic of the Langmuir isotherm is expressed in terms of a dimensionless equilibrium parameter (R_L), defined by Eq. 4:

$$R_L = \frac{1}{1 + K_l C_O} \quad (4)$$

where, C_o is the initial concentration of metal ions (mg/L). Based on the R_L, the value of $R_L > 1$ implies that the model is unfavorable, if $0 < R_L < 1$ the model is favorable, $R_L = 1$ shows the model is linear, and $R_L = 0$ introduces an irreversible model (Malise et al. 2020). Langmuir model does not present information about heterogeneous adsorption and

surface roughness (Dowlatshahi et al. 2014). Then, the Freundlich model explains the multilayer process and even the roughness of external layers. The linear form of the model is depicted in Eq. 5.

$$\mathrm{Ln}\, q_e = \mathrm{Ln}\, k_f + \left({}^{1}/_{n_f}\right)\mathrm{Ln}_{C_e} \quad (5)$$

where, k_f and n-Freundlich constant are related to the adsorption capacity and intensity, respectively. The intercept and slope value of q_e versus Ln C_e plot is used to estimate k_f and n values. If $0 < {}^{1}/_{n} < 1$ is non-linear, n = 1 is linear, n > 1 is chemical, and n < 1 is the physical adsorption process (Geremew and Zewde. 2022).

According to Table 4, R^2 indicates that the adsorption data fitted the Freundlich adsorption isotherm perfectly. The Freundlich adsorption isotherm is frequently applied to explore the adsorption performance for the heterogeneous surface and undertake multilayer adsorption. In this study, the uptake of metal ions involved in multi-molecular layer adsorption and the exterior layer was relatively heterogeneous.

Table 4. Evaluation of adsorption isotherms at ambient temperature.

Langmuir isotherm			Freundlich isotherm		
	Pb^{2+}	Cd^{2+}		Pb^{2+}	Cd^{2+}
q_m, mg/g	102.04	29.498	n_f	0.888	0.706
R_L	0.61	0.38	1/n	1.12	1.41
k_l	0.0209	0.0535	k_f	2.005	1.202
R^2	0.9198	0.9106	R^2	0.9974	0.992

Noticeably, the values of R_L of both metals are alternating from 0 to 1, revealing that the adsorption was acceptable, and it was suitable for both material eliminations.

3.5. Adsorption kinetic

The study of the adsorption kinetic provides valuable information on the adsorption rate, the adsorbent performance, and the mass transfer mechanisms. Hence, the adsorption kinetic is vital for designing suitable systems (Bayuo et al. 2020). The adsorption mass transfer kinetic has three stages, including exterior diffusion, internal diffusion, and entrance inside the active sites.

The most widely used adsorption kinetic models are the pseudo-first-order (PFO) model and the pseudo-second-order (PSO) model in the linear regression form for the simple description of adsorption parameters (Park et al. 2015). PFO varied under Henry regime adsorption (Eq. 6):

$$\frac{dq_t}{dt} = k_1\,(q_e - q_t) \quad (6)$$

where, q_t is the heavy metal adsorption capacity at time t (mg/g), q_e is equilibrium adsorption capacity (mg/g), and K_1 is the constant rate per min. It is also vital that in the PFO model, parameter K_1 is frequently used to describe how fast the adsorption equilibrium is accomplished. The integral of this equation from t =0 to t = t and q_t = 0 and $q_t = q_e$ produces a linear presence of PFO, and the linearized formula is shown in Eq. 7 (Guo and Wang 2020):

$$\mathrm{Log}(q_e - q_t) = \mathrm{Log}\, q_e - k_1 * t \quad (7)$$

PSO model undertakes that the adsorption rate of solute is related to the accessible adsorbent sites. So, the reaction degree is vastly reliant on the volume of solute on the adsorbent surface. The dynamic force (q_e _ q_t) is relative to the sum of active sites accessible on the adsorbent (Darweesh et al. 2022). The curvilinear and linear forms of PSO are presented below (Eq. 8 – Eq. 9):

$$\frac{dq_t}{dt} = k_2\,(q_e - q_t)^2 \quad (8)$$

$$\frac{t}{q_t} = \frac{1}{k_2 \times {q_e}^2} + \frac{t}{q_e} \quad (9)$$

The PSO constants are determined from a graph of t/qt vs. t (Fig. S3). The PSO model might be affected by pH, the adsorbent dosage, unit mass, and temperature, so the model calculates the impression of evident rate parameters (Nandiyanto and Ragadhito 2021). In some cases, the experimental data fit PSO better. The adsorption mechanism might be chemisorption, because of the electron transmission between the adsorbate and adsorbent. This deduction is uncertain, as the adsorption mechanism cannot be based on the modest fitting of the PSO model. It is also important that when *t* approaches zero, the PSO model would approaches the PFO model (Fig. S3) (Bayuo et al. 2020). It suggested that the pseudo-second-order model could describe the whole adsorption process of Cd and Pb. There are comparable results in other studies (Tang et al. 2017).

Intra-particle diffusion (IP) model is broadly applied to observe the limiting frequency section through adsorption. The contaminant uptake in a solution contains the adsorbate mass transfer (film diffusion), surface diffusion, and pore diffusion. The IP model reflects the significance of the diffusion phenomenon during adsorption and describes the movement of metal ions from the solution to the solid stage (composite surface) (Mirzaee and Sartaj, 2022). Film diffusion is a liberated phase, where surface and pore diffusion might coincide (Kajjumba et al. 2013). Its equation is expressed as follows (Eq. 10):

$$q_t = k_d\sqrt{t} + C \quad (10)$$

where, k_d is a rate constant (mg/g.min$^{0.5}$), and C is the boundary layer depth. The value of C limits the border layer effect, and more significant quantities show a better impact. The scheme of q_t vs $\sqrt{t}$ gives a linear function. If the straight line passes through sources, IP diffusion controls the adsorption process (Nandiyant and Ragadhito 2021). Occasionally, the plot does not move through the derivation and gives multiple linear units. Each unit corresponds to a different mechanism that controls the adsorption procedure (Fig.S4).

Three main mechanisms define the solute transfer from a solution to the adsorbent. The first one is the mass transfer (bulk movement), which starts when solute items of the adsorbent are released into the solution. This procedure is so speedy that it does not measure throughout the kinetic systems plan.

The second section is film diffusion, which includes the gentle movement of solutes from the border layer to reach the surface of the adsorbent. When the solute arrives on the external layer, they transfer to the holes of the adsorbent. The last mechanism contains a quick adsorptive attachment of the solute on the active sites inside the holes (Malise et al. 2020). Another scheme that controls the transition of particles from the liquid part to the composite surface is named liquid film diffusion. The film diffusion mechanism is evaluated by the following formula (Eq. 11):

$$\mathrm{Ln}\,(1 - F) = -k_f \times t \quad (11)$$

F is the fractional achievement of equilibrium ($F = q_t/q_e$), and K_f is the film diffusion rate constant. A linear plot with zero intercepts suggests that the adsorption kinetic is under the control of the diffusion mechanism (Argun et al. 2007). For evaluating the adsorption kinetics, the removal parameters were considered for contact times alternating from 1 to 60 minutes by checking the amount of metal ion uptake (Ren et al. 2018). The initial phase of adsorption was fewer than 60 minutes identified in previous sections, and the longer duration caused an excessive change (Fig. S5). Based on the final results in Table 5, the pseudo-second-order (PSO) model is more appropriate for the uptake of both metals.

Table 5. Calculation of kinetic parameters.

Kinetic Models	q_t, mg/g		k		R^2	
	Pb^{2+}	Cd^{2+}	Pb^{2+}	Cd^{2+}	Pb^{2+}	Cd^{2+}
pseudo-first-order (PFO) model	3.69	1.304	0.0101	0.0125	0.9163	0.9628
pseudo-second-order (PSO) model	33.589	34.29	0.068	0.066	0.9999	0.9999
Intra-particule diffusion (IP) model	29.92	32.94	0.5043	0.181	0.9255	0.9545

The R^2 of all models was more than 0.9 for Cd^{2+} and Pb^{2+}. Therefore, these models were indeed appropriate for experimental data. The fitted Cd^{2+} results for the IP model were higher, and the values of liquid film diffusion are slightly lower. It might be a reason for fractional differences in the dominant mechanism for the removal of two metals.

3.6. Determination of adsorption thermodynamics

For valuing temperature effects, calculating thermodynamic factors, including Gibbs free energy, enthalpy, and entropy are required (Imran Ali et al. 2018). The amount of ΔG and ΔS are suitable for the estimation of procedure type or influence of energy on the process that demonstrates the tendency of higher temperature (Argun et al. 2007). Eq.12 is obtained for the adsorption process:

$$\Delta G = -\,RT\,\mathrm{Ln}\,Kc \quad (12)$$

R is the ideal gas constant (kJ/mole. K), and T is the temperature in Kelvin. For calculating K_c values, the amount of concentration is necessary as $\{ Kc = \frac{C\,ad}{C_e} \times \frac{V}{m} \}$. In that case, C_e (mg/L) is the metal concentration in the equilibrium phase**,** V(L) is the solution volume, and m(g) is the amount of adsorbent added to the solution (Argun et al. 2007). The calculation of Ln Kc (Eq.13) is essential before the equilibrium as it is used for estimating ΔH and ΔS.

$$\text{Ln } Kc = \frac{\Delta S^\circ}{R} - \frac{\Delta H^\circ}{RT} \quad (13)$$

ΔH is a pattern for evaluating energy barriers during the process. The positive values of ΔH reveal the endothermic nature of the process. Then, the negative values indicate the exothermic adsorption process. As identified by many researchers, the negative value of ΔG with a positive ΔH value shows the spontaneous and endothermic nature of the process. More negative standards of ΔG at higher temperatures show that by increasing temperature, the efficiency of the process has improved considerably (Bannov et al. 2021). As a result, the dispersal of revolving and translational energy between a small number of molecules will grow with the increase of the adsorption. Therefore, a positive value of ΔS will increase at the solid–solution interface during the process. Therefore, Adsorption is probably occurring spontaneously at average and high temperatures because ΔH> 0 and ΔS>0 (Argun et al. 2007). In order to describe the adsorption kinetics of heavy metal ions, the kinetic parameters for the adsorption process were calculated for contact times ranging from 1 to 60 min by observing the removal rate of the heavy metals through the adsorbent (Table 5 – Fig.16). The enthalpy (ΔH) and entropy change were calculated from a plot of Ln kc vs. 1/T also displayed in Fig.16.

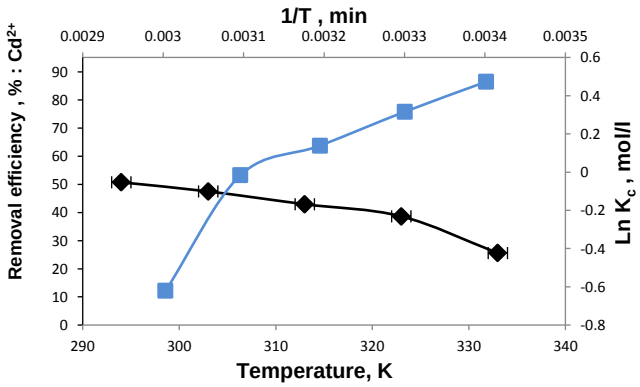

(a)

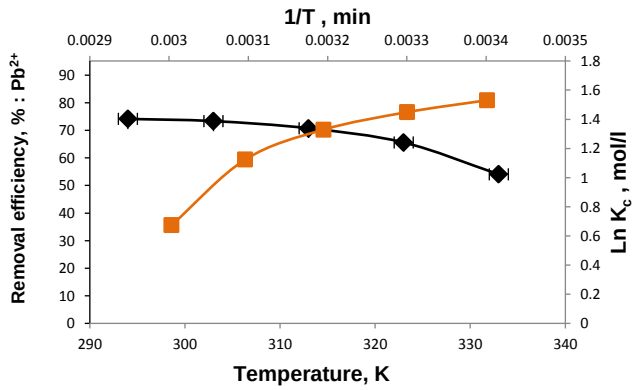

(b)

Fig.16. Evaluation of thermal elements for Cd^{2+}(a) - Pb^{2+}(b) with initial concentration=30 mg/l, pH=5, contact time =60 min.

Generally, ΔS more than zero resulted from an increment in the random adsorption that might be related to the structure change of carbonic composite and metal ions during the procedure or releasing H^+ from the adsorbent. Additionally, the positive value of ΔS in Table 6 exposed a great disturbance in the solid-solution interface during the operation. The results showed that the composite's uptake of Pb^{2+} and Cd^{2+} was spontaneous and endothermic.

Table 6. Thermodynamic parameters for adsorption of metal ions of Cd^{2+}- Pb^{2+} by the adsorbent.

		Temperature, K		
		294	303	313
ΔG, J/mole	(Cd^{2+})	-1155.03	-795.678	-359.433
	(Pb^{2+})	-3742.26	-3650.27	-3458.79
ΔS, J/mole.K	(Cd^{2+})		43.6377	
	(Pb^{2+})		65.9309	
ΔH, J/mole	(Cd^{2+})		20760.1	
	(Pb^{2+})		16814.2	

3.7. Reusability of adsorbent

The reusability of new composites is a substantial factor for estimating their practicability in real-world applications since effective repetitive disposal of adsorbent will diminish the general cost of the adsorption process. Excluding the adsorption capacity of the adsorbents, the desorption and reusability of the adsorbent resources are similarly convincing parameters for adsorption removal efficiency.

Nanostructure adsorbents can be recycled and continually used, which makes them cost-effective and highly attractive for treatment purposes (Wadhawan et al. 2019). Any adsorbent with higher adsorption capacity and better desorption properties will decrease the overall cost of the treatment, which is particularly important for industrial practice (Zhang et al. 2019).

It was reused in consecutive experiments to study the reusability of the composite. The used adsorbents were washed with acid (HCL) and deionized water to remove metal ions altogether and then reused to adsorb Cd^{2+} and Pb^{2+} in 50 mL of the solution. The recycling process was repeated with a similar method five times, and all stages of Cd^{2+} and Pb^{2+} in the solutions were measured after removing the composite (Fig.17) (Tang et al. 2017).

The adsorbent has the potential to be reused, accompanied by being an economical and straightforward way to remove low concentrations of metal ions. According to the results, the rate of desorption capacity was condensed during the following cycles. The removal efficiency was less than primary uses, and the pH of the desorption process was harmfully related to the pH effect in the adsorption process.

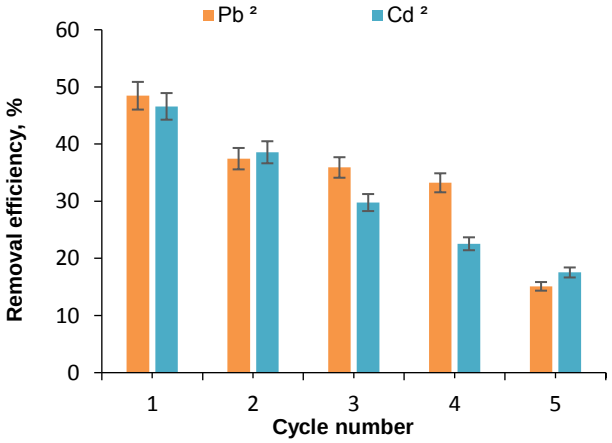

Fig. 17. Uptake calculating after 5-time recycling at optimum condition (pH=5, Contact time=60 min, adsorbent dosage=2 g/l, at ambient temperature).

3.8. Comparison of the prepared absorbent with others in the literature

Up to now, various adsorbents have been used to remove lead and cadmium from water sources. Table 7 provides information about different adsorbents and their adsorption capacity for evaluating the efficiency of the prepared adsorbent in this study and comparing it with other adsorbents in the literature. The maximum adsorption capacity of 102.04 mg/g for Pb^{2+} is suitable, demonstrating that this composite can be used for lead elimination.

Table 7. Comparison of adsorption capacity (q_m) of carbon-based adsorbents.

Adsorbent	Metal ions	q_m (Langmuir) mg/g	References
Water hyacinth BC	Cd^{2+}	70.3	
Oxidized MWCNTs		2.67−11.70	Duan et al. 2020
β-cyclodextrin modified magnetic GO	Pb^{2+}	279.21	
EU-biochar		200	Shafiq et al. 2021
Rice husk biochar	Pb^{2+}	1.84	
Buffalo weed biochar		333.3	
WTPC	Pb^{2+}	23.42	Malise et al. 2020
WTAC		85.91	
TC :(Typha angustifolia activated carbon)	Cd^{2+}	48.08	
	Pb^{2+}	61.73	
SC :(Salix matsudana activated Carbon)	Cd^{2+}	40.98	Tang et al. 2017
	Pb^{2+}	58.82	
CAC :(commercial activated carbon)	Cd^{2+}	56.82	
	Pb^{2+}	70.42	
(3-MPA@PMNPs)	Cd^{2+}	79.8	Imran Ali et al. 2018
	Pb^{2+}	68.41	
activated carbon prepared from saffron leaves	Cd^{2+}	68.75	Dowlatshahi et al. 2014
	Pb^{2+}	79.6	
EG/ g-C_3N_4 / Phenylenediamine	Cd^{2+}	29.49	This work
	Pb^{2+}	102.04	

4. Conclusions

In summary, a new EG/g-C_3N_4/phenylenediamine composite was prepared to remove Cd^{2+} and Pb^{2+} from aqueous solutions. The prepared adsorbent was optimized using Design-Expert. The ANOVA analysis of adsorbent optimization showed appropriate stability between the experimental and expected values (model $P<0.005$, R^2=92.29%). The SEM, FESEM, EDS, and BET analyses studied the morphological and structural characterization of the adsorbent. The preparation of g-C_3N_4 from melamine and phenylenediamine created a white cover on the graphite outer layers. The uptake percentages of both metals were partially different. The main factor affecting the removal efficiency of the process was pH. The equilibrium occurred quickly before 60 minutes, and the proper pH value was less than 6 for both contaminants. The maximum removal rate was 78% for Cd^{2+} and 70.4% for Pb^{2+}, obtained in pH=5, T=60 minutes with 2 g/L of the adsorbent at ambient temperature. The isotherm adsorption study showed that experimental data were fitted with the Freundlich model with suitable removal efficiency. The maximum adsorption capacity for Pb^{2+} and Cd^{2+} were 102.04 and 29.49 mg/g, respectively. The kinetic study showed that the removal process might be under the control of the liquid diffusion mechanism at the initial phase, and the pseudo-second-order (PSO) model was more appropriate. The thermodynamic evaluation indicated that this composite's adsorption of Pb^{2+} and Cd^{2+} was spontaneous and endothermic. The final product showed a capable adsorbent in low ranges of heavy metal uptake. Based on the results, developing carbon-based materials can be promising for heavy metal removal from water sources.

Acknowledgment

The authors want to thank the School of Environment, College of Engineering, University of Tehran, Iran, for providing the laboratory equipment and supplementary materials. The authors also appreciate Kish International Campus of Tehran University, Iran, for their support.

References

Abbas A., Ajaz H.M., Sher M., Irfan M.I., Design, characterization and evaluation of hydroxyethyl cellulose based novel regenerable super sorbent for heavy metal ions uptake and competitive adsorption, International Journal of Biological Macro Molecules 102 (2017) 170 – 80.

Abdulkarim M., and Al-Rub F.A., Adsorption of lead ions from aqueous solution onto activated carbon and chemically-modified activated carbon prepared from date pits, Adsorption Science & Technology 22 (2004) 119-134.

Argun M., Emin A., Dursun S., Heavy metal adsorption by modified oak sawdust: Thermodynamics and kinetics, Journal of Hazardous Materials 141 (2007) 77–85.

Bannov A.G., Ukhina A.V., Maksimovskii Evgenii A., Prosanov Igor Yu., Shestakov Artyom A., Lapekin Nikita I., Highly porous expanded graphite: thermal shock vs. programmable heating, Materials 14 (2021) 7687.

Bayuo J., Abdullai A.M., Bayetimani K., Optimization using central composite design (CCD) of response surface methodology (RSM) for biosorption of hexavalent chromium from aqueous media, Applied Water Science 10 (2020) 1-12.

Burakov A., Romantsova I., Kucherova A., Tkachev A. Removal of Heavy-metal Ions from aqueous solutions using activated carbon: effect of Adsorbent Surface Modification Wit Carbon Nanotubes, Tambov State Technical University 32 (2014) 737-747.

Celzard A., Marêché J.F., Furdin G., Modelling of exfoliated graphite, Progress in Materials Science 50 (2005) 93–179.

Chakraborty R., Anupama A., Ajaya K.S., Adsorption of heavy metal ions by various low-cost adsorbents: a review, International Journal of Environmental Analytical Chemistry 102 (2022) 342-379.

Chen X., Modeling of experiential adsorption isotherm data, Information 6 (2015) 14-22.

Cruz-Lopes L.P., Macena M., Esteves B., Guiné R.P.F., Ideal pH for the adsorption of metal ions Cr^{6+}, Ni^{2+}, Pb^{2+} in aqueous solution with different adsorbent materials, De Gruyter 6 (2021) 115–123.

Darweesh M.A., Elgendy M.Y, Ayad M.I, Ahmed A., Adsorption isotherm, kinetic, and optimization studies for copper (II) removal from aqueous solutions by banana leaves and derived activated carbon, South African Journal of Chemical Engineering 40 (2022) 10–20.

Dowlatshahi Sh., Haratinezhad T.A.R., Loloei M., Adsorption of copper, lead and cadmium from aqueous solutions by activated carbon prepared from saffron leaves, Environmental Health Engineering and Management Journal 1 (2014) 37–44.

Duan C., Ma T., Wang J., Zhou Y., Removal of heavy metals from aqueous solution using carbon-based adsorbents: A review, Journal of Water Process Engineering 37 (2020) 101339.

Farimaniraad H., Pardakhti A., Kalarestaghi H., Carcinogenic and non-carcinogenic health risk assessment of heavy metals in ground drinking water wells of Bandar Abbas, Pollution 7 (2021) 395-404.

Fergusson L., Three novel methods for removing inorganic species from contaminated industrial storm water at a Smelter site in London, Journal of Applied Research in Water and Wastewater 3 (2015) 115-121.

Falsafi M.H., Moghaddas M., Moghaddas J.S., Removal of heavy metals from synthetic wastewater using silica aerogel- activated carbon composite by adsorption method, Journal of Applied Research in Water and Wastewater 13 (2020) 89-95.

Geremew B., and Zewde D., Hagenia abyssinica leaf powder as a novel low-cost adsorbent for removal of methyl violet from aqueous solution: Optimization, isotherms, kinetics, and thermodynamic studies, Environmental Technology & Innovation 28 (2022) 102577.

Głowacz C.D., Prospects of using melamine solutions in reactive solvents in polymer technology, Rzeszów University of Technology, Rzeszów 67 (2013) 289-300.

Gupta M., Savla N., Pandit C., Pandit S., Gupta P.K., Pant M., Khilari S., Kumar Y., Agarwal D., Nair R.R., Thomas D., Thakur V.K., Use of biomass-derived biochar in wastewater treatment and power production: A promising solution for a sustainable environment, The Science of the total environment, 825 (2022) 153892.

Hadiani M.R., Khosravi K., Rahimifard N., Younesi H., Biosorption of low concentration levels of Lead (II) and Cadmium (II) from aqueous solution by Saccharomyces cerevisiae: Response surface methodology, Biocatalysis and Agricultural Biotechnology15 (2018) 25-34.

Hou B., Sun H.j., Peng T.j., Zhang X.Y., Rapid preparation of expanded graphite at low temperature, New Carbon Materials 35 (2020) 262-268.

Hung W.C., Wang J.C., Wu K.H., Adsorption and decomposition of dimethyl methyl phosphonate (DMMP) on expanded graphite/metal oxides, Applied Surface Science 444 (2018) 330 – 335.

Imran Ali A., Peng C., Naz I., Removal of lead and cadmium ions by single and binary systems using phytogenic magnetic nanoparticles functionalized by 3-marcaptopropanic acid, Materials and Product Engineering 27 (2018) 949 – 964.

Jiao X., Zhang L., Qiu Y., Yuanab Y., A new adsorbent of Pb(II) ions from aqueous solution synthesized by mechanochemical preparation of sulfonated expanded graphite, RSC advances, 7(61), (2017), 38350-38359.

Jin H., Ji Z., Yuan J., Li J., Liu M., Xu C., Dong J., Research on removal of fluoride in aqueous solution by alumina-modified expanded graphite composite, Journal of Alloys and Compounds 620 (2015) 361–367.

Kajjumba G.W., Emik S., Öngen A., Özcan H.K., Modelling of adsorption kinetic processes—errors, theory and application, advanced sorption process applications, Advanced Sorption Process Applications, IntechOpen, (2018) 1 - 19.

Kheradmand A., Negarestani M., Mollahosseini A., Low-cost treated lignocellulosic biomass waste supported with $FeCl_3/Zn(NO_3)_2$ for water decolorization, *Scientific Reports*, 12(1), (2022), 16442.

Liao N., Li Y., Shan J., Tianbin Z., Improved oxidation resistance of expanded graphite through nano SiC coating, Ceramics International 44 (2017) 3319-3325.

Liu T., Zhang R., Zhang X., Liu K., One-step room-temperature preparation of expanded graphite, Carbon 119 (2017) 544-547.

Liu W., Wang T., Borthwick A.G.L., Wang Y., Yin X., Li X., Ni J., Adsorption of Pb^{2+}, Cd^{2+}, Cu^{2+} and Cr^{3+} onto titanate nanotubes: Competition and effect of inorganic ions, Science of the Total Environment, 456, (2013), 171–180.

Malise L., Rutto H., Seodigeng T., Sibali L., Ndibewu P., Adsorption of lead ions onto chemical activated carbon derived from waste tire pyrolysis char: Equilibrium and kinetics studies, Chemical Engineering Transactions 82 (2020) 421-426.

Meibodi F., and Soori E., Synthesis of magnetic nanoparticles (Fe_3O_4) coated with fatty acids and surfactants and their application in demulsification of crude oil-in-water emulsions, Journal of Applied Research in Water and Wastewater 9 (2022) 76-84.

Mirzaee E., and Sartaj M., Activated carbon-based magnetic composite as an adsorbent for removal of polycyclic aromatic hydrocarbons from aqueous phase: Characterization, adsorption kinetics and isotherm studies, Journal of Hazardous Materials Advances 6 (2022) 100083.

Mohanraj j., Durgalakshmi D., Balakumar S., Low cost and quick time absorption of organic dye pollutants under ambient condition using partially exfoliated graphite, Journal of Water Process Engineering 34 (2020) 101078.

Negarestani M., Mollahosseini A., Farimaniraad H., Ghiasinejad H., Shayesteh H., Kheradmand A., Efficient removal of non-steroidal anti-inflammatory ibuprofen by polypyrrole-functionalized magnetic zeolite from aqueous solution: kinetic, equilibrium, and thermodynamic studies, Separation and Purification Technology 58 (2022) 435-453.

Nouri S., Effect of functional groups and pH on the affinity and adsorption capacity of activated carbon: Comparison of homogeneous and binary Langmuir model parameters, Adsorption Science & Technology 21 (2003) 511-524.

Ocreto J., Go C.I., Chua J.C., Apacible C.J., Vilando A., Competitive effects for the adsorption of copper, cadmium and lead ions using modified activated carbon from bamboo, MATEC Web of Conferences, 268, (2019), 06021.

Park J.H., Ok Y.S., Kim S.H., Cho J.S., Heo J.S., Competitive adsorption of heavy metals onto sesame straw biochar in aqueous solutions, Chemosphere 142 (2016) 77-83 .

Parmar P., Shukla A., Goswami D., Patel B., Saraf M., Optimization of cadmium and lead bio sorption onto marine Vibrio alginolyticus PBR1 employing a Box-Behnken design, Chemical Engineering Journal Advances 4 (2020) 100043.

Rao M., Parwate A.V., Bhole A.G., Kadu P.A., Performance of low-cost adsorbents for the removal of copper and lead, Journal of Water Supply 52 (2003) 49 – 58.

Ren B., Xu Y., Zhang L., Liu Z., Carbon-doped graphitic carbon nitride as environment-benign adsorbent for methylene blue adsorption: Kinetics, isotherm and thermodynamics study, Journal of the Taiwan Institute of Chemical Engineers 88 (2018) 114–120.

Savaloni H., and Savari R., Nano-structural variations of ZnO:N thin films as a function of deposition angle and annealing conditions: XRD, AFM, FESEM and EDS analyses 214 (2018) 402 - 420.

Shafiq M., Alazba A.A., Tahir A. M., Kinetic and isotherm studies of Ni^{2+} and Pb^{2+} adsorption from synthetic wastewater using Eucalyptus camdulensis- Derived bio char, Sustainability 13 (2021) 3785.

Shen W., Li Z., Liu Y., Surface Chemical Functional Groups Modification of Porous Carbon. Recent Patents on Chemical Engineering 1 (2008) 27- 40.

Sun Y.p., Ha W., Chen J., Qi H.y., Shi Y.p., Advances and applications of graphitic carbon nitride as sorbent in analytical chemistry for sample pretreatment: A review, Trends in Analytical Chemistry 84 (2016) 12- 21.

Taherian R., Kausar, A., application of polymer-based composites: Bipolar plate of PEM fuel cells, Electrical Conductivity in Polymer-Based Composites, Eds, (2018), 183-237.

Tahoon M.A, Siddeeg, S. M., Salem Alsaiari, N., Mnif, W., Ben Rebah, Effective heavy metals removal from water using nanomaterials. A review:processes, 8(6), (2020), 645.

Tang C., Shu Y., Zhang R., Li X., Comparison of the removal and adsorption mechanisms of cadmium and lead from aqueous solution by activated carbons prepared from Typha angustifolia and Salix matsudana, RSC Advances 7 (2017) 16092 - 16103.

Wadhawan Sh., Jain A., Jasamrit N., Kumar M.S., Role of nanomaterials as adsorbents in heavy metal ion removal from wastewater: A review, Journal of Water Process Engineering 33 (2020) 101038.

Wang J., and Guo X., Adsorption kinetic models: Physical meanings, applications, and solving methods, Journal of Hazardous Materials 390 (2020) 122156.

Yuan W., Juan C., Hexiang H., Xiong S., Gao J., Optimization of cadmium biosorption by Shewanella putrefaciens using a Box-Behnken design, Ecotoxicology and Environmental Safety 175 (2019) 138–147.

Zhang Q., Hou Q., Huang G., Fan Q., Removal of heavy metals in aquatic environment by graphene oxide composites, Environmental Science and Pollution Research 27 (2020) 190-209.